Chinese Chemical Letters 35 (2024) 109021

Contents lists available at ScienceDirect

Chinese Chemical Letters

journal homepage: www.elsevier.com/locate/cclet

Functionalization of cellulose carbon dots with different elements (N, B and S) for mercury ion detection and anti-counterfeit applications

Xiaoning Li[a,b,1], Quanyu Shi[b,1], Meng Li[b,*], Ningxin Song[b], Yumeng Xiao[b], Huining Xiao[c], Tony D. James[d,e], Lei Feng[a,e,*]

[a] Second Affiliated Hospital of Dalian Medical University, Dalian 116023, China
[b] Hebei Key Lab of Power Plant Flue Gas Multi-Pollutants Control, Department of Environmental Science and Engineering, North China Electric Power University, Baoding 071003, China
[c] Department of Chemical Engineering and Limerick Pulp & Paper Centre, University of New Brunswick, 15 Dineen Drive, Fredericton NB E3B 5A3, Canada
[d] Department of Chemistry, University of Bath, Bath BA2 7AY, United Kingdom
[e] School of Chemistry and Chemical Engineering, Henan Normal University, Xinxiang 453007, China

ARTICLE INFO

Article history:
Received 3 July 2023
Revised 25 August 2023
Accepted 29 August 2023
Available online 2 September 2023

Keywords:
Carbon dots
Functional groups
Hg^{2+} detection
Mechanism
Anti-counterfeiting

ABSTRACT

Mercury ion (Hg^{2+}), as one of the most toxic heavy metal ions, accumulates easily in the environment, which can generate potential hazards to the ecosystem and human health. To effectively detect and remove Hg^{2+}, we fabricated four types of carbon dots (CDs) using carboxymethyl nanocellulose as a carbon source doped with different elements using a hydrothermal method. All the CDs exhibited a strong fluorescence emission, excitation-dependent emission and possessed good water dispersibility. Moreover, the four fluorescent CDs were used for Hg^{2+} recognition in aqueous solution, where the CDs-N exhibited better sensitivity and selectivity for Hg^{2+} detection, with a low limit of detection of 8.29×10^{-6} mol/L. It was determined that the fluorescence quenching could be ascribed to a photoinduced charge-transfer processes between Hg^{2+} and the CDs. In addition, the CDs-N were used as a smart invisible ink for anti-counterfeiting, information encryption and decryption. Furthermore, the CDs-N were immersed into a cellulose (CMC)-based hydrogel network to prepare fluorescent hydrogels capable of simultaneously detecting and adsorbing Hg^{2+}. We anticipate that this research will open possibilities for a green method to synthesize fluorescent CDs for metal ion detection and fluorescent ink production.

© 2024 Published by Elsevier B.V. on behalf of Chinese Chemical Society and Institute of Materia Medica, Chinese Academy of Medical Sciences.

With rapid industrial development, metal contamination is a significant issue to potable water security [1]. Among the metal ions, mercury ion (Hg^{2+}) is recognized as one of the most hazardous metal contaminants [2,3], which would pose a significant threat to human health and environmental ecology. When mercury ions enter the human body, the mercury ions will cooperate with thiol group in proteins, thus significantly affecting human mental and neurological function [4,5]. There is thus urgent need for a system capable of sensitively and efficiently detecting mercury ions in wastewater. At present, various detection techniques have been successfully developed to recognize mercury ions, such as chromatography, inductively coupled plasma-mass spectrometry, atomic fluorescence technology and electrochemistry. Among which, fluorescence sensors exhibit great potential due to their simplicity, excellent sensitivity and selectivity [6–10]. Currently, various responsive mechanisms, including intramolecular charge transfer, inner filter effect and chelation quenched fluorescence, have been employed for the detection of mercury ions.

So far, carbon dots (CDs) have received wide attention because of their excellent water solubility, low toxicity, biocompatibility, chemical stability and good energy and charge transfer properties [11–13]. Owing to these advantages, CDs are considered as promising fluorescent probes for the detection of Hg^{2+} [14–16]. However, the high-cost of the raw material and low production yield hinder the development of industrial applications of CDs. Recently, a variety of raw biomass materials (juice, grapefruit peel, rice husk, *etc.*) have been used as carbon precursors to address these issues. Cellulose, the most abundant natural biomass on the earth, is renewable, non-toxic, completely biodegradable, and exhibits excellent biocompatibility [17–19]. It represents a promising and inexhaustible raw material for the preparation of carbon nanomaterials that could realize the sustainable future development of human society. More importantly, the synthesized CDs from carboxymethyl nanocellulose (C-CNC) possess abundant carboxyl

* Corresponding authors.
E-mail addresses: mlincepu@hotmail.com (M. Li), leifeng@dmu.edu.cn (L. Feng).
[1] These authors contributed equally to this work.

https://doi.org/10.1016/j.cclet.2023.109021
1001-8417/© 2024 Published by Elsevier B.V. on behalf of Chinese Chemical Society and Institute of Materia Medica, Chinese Academy of Medical Sciences.

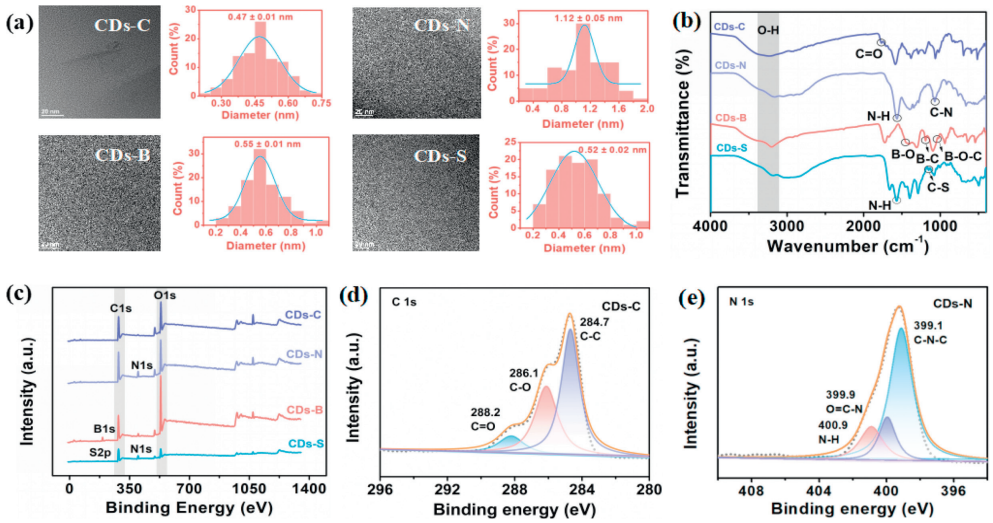

Fig. 1. Characterization of CDs-C, CDs-N, CDs-B and CDs-S. (a) Transmission electron microscopic (TEM) images and particle size distribution of CDs-C, CDs-N, CDs-B and CDs-S. Scale bar: 20 nm. (b) FT-IR spectra of CDs-C, CDs-N, CDs-B and CDs-S. (c) XPS survey spectrum. (d) High resolution XPS spectra of C 1s of CDs-C. (e) The N 1s spectra of CDs-N.

groups, offering the potential for chemical modification. Recent research has reported on various carboxymethyl nanocellulose-based CDs with excellent biodegradability, compatibility and optical properties [20,21]. However, the existing cellulose-based CDs are still largely underdeveloped with a bottleneck generated by the low quantum yield and the limited fluorescence sensing capacity. Notably, the CDs doped with the N, B, S and other elements can effectively tune the photoluminescence properties and enhance the quantum yield [22–24]. Moreover, CDs doped with different elements contain abundant functional groups on their surfaces, which can improve the sensitivity for metal ions [25]. We thus expected that the nanocellulose-based CDs could be further modified with various functional groups for enhanced optical performance and sensing properties.

With this research, a series of CDs including CDs containing carboxyl groups (CDs-C), amine-modified CDs (CDs-N), boron oxygen-modified CDs (CDs-B) and sulfhydryl-modified CDs (CDs-S) were prepared using a one-pot hydrothermal method. As expected, the four CDs display a visible blue emission and excitation-dependent properties. Moreover, the four CDs as sensors were employed to detect Hg^{2+}. Notably, the CDs-N exhibited excellent sensitivity and selectivity for Hg^{2+} compared with other functional group modified CDs. Density functional theory (DFT) calculations confirmed that the high binding energy of CDs-N to Hg^{2+} and charge transfer between spatially separated amine groups contribute to the strong fluorescence quenching. The CDs-N was used as a fluorescent ink for anti-counterfeit printing. Furthermore, CDs-N was successfully encapsuled into a hydrogel for the detection and removal of Hg^{2+}.

Four types of CDs were prepared *via* a hydrothermal treatment method using C-CNC as the carbon source. As shown in Fig. 1a, all samples demonstrate a typical spherical shape and a good dispersity in aqueous solution. The average size of the synthesized CDs-C, CDs-N, CDs-B and CDs-S were determined to be 0.47, 1.12, 0.55 and 0.52 nm, respectively. Moreover, the chemical structure and composition of four CDs were measured using Fourier transform infrared (FT-IR) analysis. In Fig. 1b, the CDs-C show the -OH stretching vibrations at 3300 cm^{-1} and the characteristic band of C=O at 1771 cm^{-1}, which indicates the presence of carboxylic acid groups on the CDs-C. The stretching vibrations peak of -NH_2 and C-N on CDs-N are found at 1569 and 1070 cm^{-1}, respectively [26]. For the CDs-B, the emergence of peaks at 1030, 1190 and 1450 cm^{-1} imply the presence of the B-O-C, C-B and B-O bonds [27]. It was also found C-S stretching vibrations at 1153 cm^{-1} in the CDs-S. These FT-IR analyses confirmed that the -NH_2, B-O bond and -SH groups are successfully loaded on the CDs. Furthermore, the presence of carboxyl groups on CDs-N, CDs-B, and CDs-S was found to be inconspicuous. The incorporation of distinct functional groups into CDs enables diverse detection outcomes when applied to different samples. To further confirm the above FT-IR results, the X-ray photoelectron spectrum (XPS) of the CDs-C, CDs-N, CDs-B and CDs-S were also investigated. In the XPS spectrum, the C, O, N, B and S elements can be observed in the four different CDs (Fig. 1c). The C 1s spectra of CDs-C can be divided into three peaks at 284.7, 286.1 and 288.2 eV, which corresponded to C-C, C-O and C=O bonds, respectively (Fig. 1d). The result demonstrated the existence of carboxyl group on the CDs-C. After modification, the slight change of C 1s can be seen (Fig. S1 in Supporting information). For the CDs-N, the C 1s showed three components that are assigned to C-C (284.6 eV), C-O/C-N (285.9 eV) and C=O (287.8 eV) bonds (Fig. S1a in Supporting information). The difference in C 1s of 288.7 eV (C=O/C-O-B) in the CDs-B and 285.6 eV (C-O/C-N/C-S) in the CDs-S were observed (Figs. S1c and e in Supporting information). The observed difference of four CDs further suggested that the reaction between the C-CNC and different functional groups. For the CDs-N, the N 1s reveal the presence of C-N-C (399.1 eV), O=C-N (399.9 eV) and N-H (400.9 eV) groups, which further suggests the successful reaction of the urea with the carboxyl group in C-CNC (Fig. 1e) [28]. Based on the above experimental evidence, it can be deduced that the four CDs possess different functional groups, which can generate different fluorescence and sensing properties.

Subsequently, the photophysical properties of four CDs were examined in detail. As shown in Figs. 2a–d, the ultraviolet-visible (UV-vis) spectra displayed a peculiar absorption band in the range of 200–300 nm for the four types of CDs, which may be related to the π-π^* transitions. The weak absorption shoulder at 300–450 nm is related to the n-π^* transition of C=O on the surface [25]. The observations confirm that the functional surface states can produce different energy states. Moreover, the four solutions of CDs exhibited a bright blue fluorescence under UV light. All CDs displayed a strong fluorescence emission at 434-437 nm under excitation at 360 nm. Furthermore, CDs-C, CDs-N, CDs-B and CDs-S displayed excitation-dependent properties, with emission maxima at 438, 435, 437 and 452 nm, respectively, under the optimal excitation wavelength of 360 and 380 nm (Figs. 2e–h). The fluores-

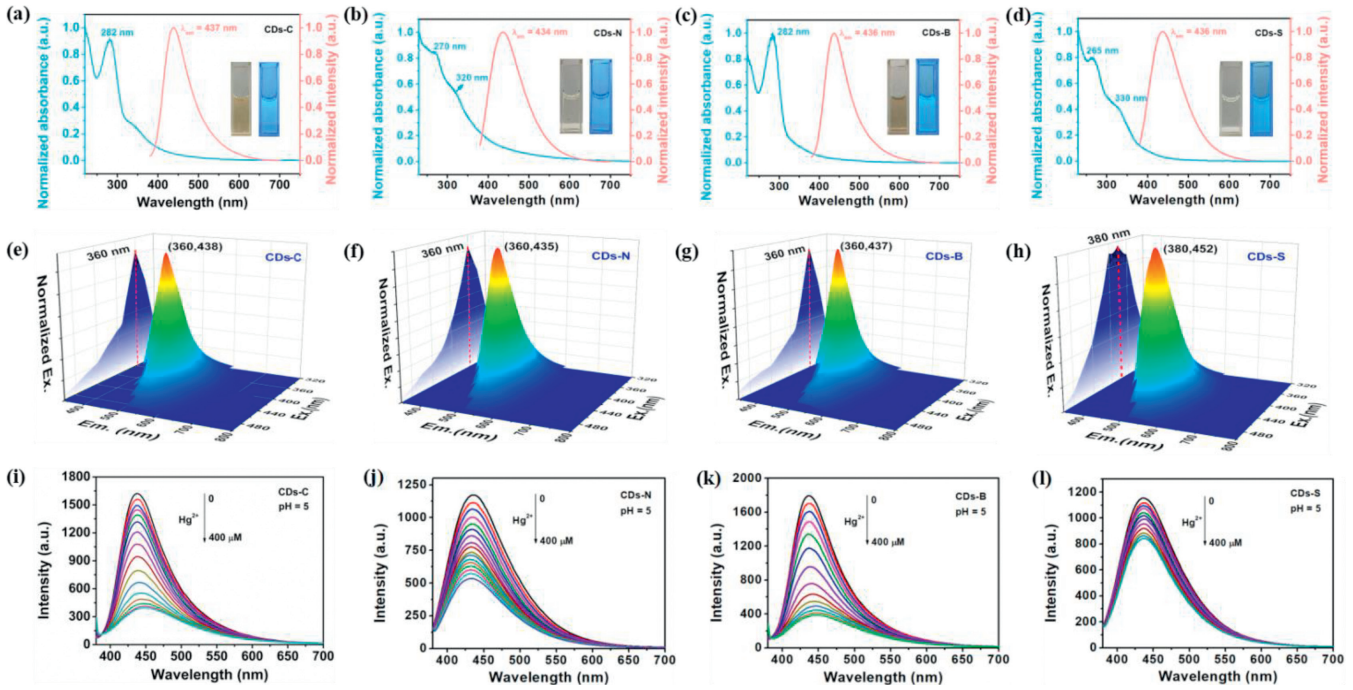

Fig. 2. Fluorescence properties of CDs-C, CDs-N, CDs-B and CDs-S. (a–d) Normalized absorbance and intensity of CDs-C, CDs-N, CDs-B and CDs-S (insert: images of CDs-C, CDs-N, CDs-B and CDs-S solutions under UV irradiation). (e) The 3D fluorescence spectra of CDs-C, (f) CDs-N, (g) CDs-B and (h) CDs-S at different excitation wavelengths. (i–l) Fluorescence response of the CDs-C, CDs-N, CDs-B and CDs-S (0.25 mg/mL) with different concentrations of Hg^{2+} (0–400 μmol/L) ($\lambda_{ex} = 360$ nm).

cence tunability of four types of CDs is presumably due to the inhomogeneity of the particle sizes and the numerous emissive traps of surface states formed by the -OH, -COOH, -NH_2, B-O bond and -SH functional groups. Moreover, the relative quantum yield of the CDs-C, CDs-N, CDs-B and CDs-S were determined to be 0.98%, 2.8%, 1.25% and 10.46%, respectively.

To further explore the fluorescence mechanism, the four CDs were used to detect Hg^{2+}. Upon the addition of Hg^{2+}, the fluorescence intensity of the CDs-C showed a significant decreased under 360 nm excitation (Fig. 2i). Simultaneously, the CDs-N, CDs-B and CDs-S also displayed a similar fluorescence quenching in the presence of Hg^{2+} (Figs. 2j–l). By calculating the emission intensity ratio of I_0/I *versus* the concentration of Hg^{2+} (0–100 μmol/L), an excellent linear response was obtained with $R^2 = 0.988$ (Fig. S2a in Supporting information). The detection limit of the CDs-C, CDs-N, CDs-B and CDs-S were calculated to be 1.95×10^{-5} mol/L, 8.29×10^{-6} mol/L, 1.05×10^{-5} mol/L and 2.53×10^{-5} mol/L based on 3 δ/k (where δ stands for the standard deviation of the blank four CDs solutions, and k is the slope of the linear plots.), showing a good sensitivity for Hg^{2+} [29]. In addition, four types of CDs showed a great selectivity for Hg^{2+} (Fig. S3 in Supporting information). These results indicate that energy transfer can occur between the CDs and Hg^{2+} in solution, thus resulting in a distinct fluorescence quenching. For comparison, it was found that the CDs-N exhibit a better detection capability toward Hg^{2+}. The fluorescence lifetimes and zeta potential of four CDs indicate that a high affinity between the amino group on the CDs-N and the Hg^{2+} may contribute to the excellent fluorescence performance (Fig. S4 and Table S1 in Supporting information). Meanwhile, the pH investigation further confirmed that the applicability of CDs-N for Hg^{2+} (Fig. S5 in Supporting information).

In order to further understand the luminescence and detection mechanism of the four CDs, molecular modelling based on DFT was performed. The proposed structure for the four CDs is a single layer graphene as the carbon core (Fig. S6 in Supporting information). It can be seen that the functional groups functionalized coronene models exhibit a planar structure, and the electron pair on functional groups and the π orbital of coronene formed a big conjugated π orbital, generating interactions with the Hg^{2+} ions. The distances between Hg^{2+} and the carboxyl (-COOH), amino (-NH_2), boron oxygen (-B-O) and sulfhydryl (-SH) groups of the four CDs were 3.636, 3.604, 3.578 and 2.645 Å, respectively, indicating that the interactions existed among CDs with mercury ions. In addition, the corresponding binding energies (BE), Mulliken charges of Hg^{2+} as well as the charges transfer from four CDs to Hg^{2+} were calculated (Table S2 in Supporting information). Notably, the BE of CDs-N/Hg^{2+} is calculated to be −357.43 kcal/mol, which is much higher than the other three complexes with BEs values ranging from −346.94 kcal/mol to −356.47 kcal/mol. The excellent BE of CDs-N/Hg^{2+} indicated that the -NH_2 on the surface of CDs-N have a higher affinity for Hg^{2+}. Moreover, the superior charge transfer from CDs-N to Hg^{2+} (2.011) further confirmed that the CDs-N preferred to form stable complexes with Hg^{2+} rather than the other three CDs. The above results revealed that the CDs-N can preferentially detect Hg^{2+} over the other three CDs, which was in good agreement with the fluorescent selectivity and sensitivity of the CDs for Hg^{2+}.

The identification of the charge transfer process between functional groups and Hg^{2+} ions as a quenching mechanism for fluorescence CDs provides a powerful toolbox for a better understanding of their use in technological applications. Inspired by the excellent optical properties, the prepared CDs-N can be applied in diverse applications including anti-counterfeiting, sensing and adsorption of metal ions.

These high-performance CDs-N with excellent photostability exhibit great potential for anti-counterfeiting applications. The experiment is carried out using a pen with an aqueous solution of CDs-N as the fluorescent ink (Fig. 3a). In Fig. 3a, the CDs-N were used and painted on a hybrid filter membrane for investigating the anti-counterfeiting properties. The rich surface functional groups confer the CDs-N with good adhesion to the hybrid filter membrane, and hence diverse fine patterns (watering cans, clouds, butterflies and

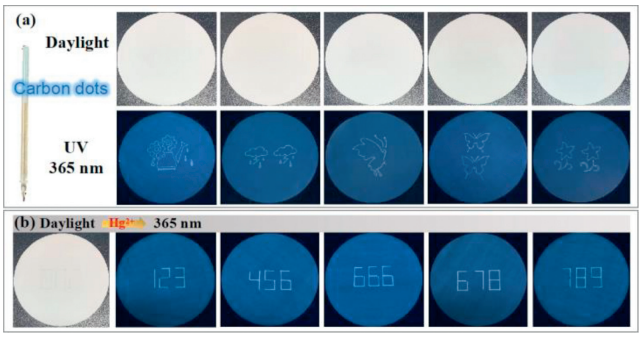

Fig. 3. Anti-counterfeiting application of CDs-N. (a) Images of printed patterns on hybrid filter membrane for CDs-N. (b) Images of information encryption using the CDs-N ink in daylight and under UV light.

flowers) were obtained by writing with a pen (Fig. 3a). It can be clearly observed that these patterns are basically colorless and invisible in sunlight, while exhibiting a bright blue light under UV irradiation. Encouraged by the excellent properties, CDs-N aqueous was coated on a hybrid filter membrane for information encryption under daylight and information decryption under UV light (Fig. 3b). The numeral "888" is hand-drawn using a fountain pen and visible under daylight. Remarkably, even when a portion of the numeral "8" is entirely covered with Hg^{2+} solution and allowed to dry, the displayed numeral under daylight remains unchanged as "888". However, under 365 nm ultraviolet excitation, distinct numerals such as "123", "456", "666", "678", and "789" become discernible. These results again corroborate the strong quenching effect of Hg^{2+} on CDs-N and highlights the remarkable potential of CDs-N for highly effective anti-counterfeiting applications. In addition, the fluorescence code can also be achieved using a smart phone. As shown in Fig. S7 (Supporting information), the quick response (QR) code on the filter paper displayed a bright blue QR code under UV irradiation.

Moreover, the QR code produced no information under daylight, while the stored message "carbon dots" can be obtained by scanning with a smartphone under UV irradiation, suggesting that the information could be encrypted multiple times and transmitted using this material. These results confirmed that the anti-counterfeiting technology with CDs-N can provide a promising application in the field of high-level security.

Inspired by the sensing properties of CDs, the four CDs were encapsuled into a cellulose-based hydrogel by hydrogen bonding to prepare fluorescent hydrogels for the simultaneous detection and adsorption of Hg^{2+} ions [30,31]. As shown in Fig. 4a, the scanning electron microscope (SEM) images confirmed that the cellulose-based hydrogel exhibited a porous structure and three-dimensional network, which would provide numerous adsorption sites for the removal and detection of Hg^{2+} ions. Moreover, energy-dispersive X-ray spectroscopy (EDS)-mapping indicates uniform dispersion of C, O and N elements in the cellulose-based hydrogel, suggesting that the hydrogel contains various functional groups for the adsorption of metal ions (Fig. 4b). The fluorescent hydrogels were prepared by immersing the four CDs into a cellulose-based hydrogel network for the sensing and removal of Hg^{2+} (Fig. 4c). As shown in Fig. 4d, the sodium carboxymethyl cellulose/CDs-N (CA/CDs-N) hydrogel exhibits a fluorescence quenching upon the addition of the Hg^{2+}. Similar fluorescence quenching was observed for the CA/CDs-C, CA/CDs-B and CA/CDs-S hydrogels (Fig. S8 in Supporting information). A linear response of four fluorescent hydrogels toward Hg^{2+} was observed (Fig. 4e). The detection limit of four fluorescent hydrogels were calculated to be 8.53×10^{-5}, 4.73×10^{-5}, 9.01×10^{-5} and 2.51×10^{-4} mol/L, respectively. Particularly, the CA/CDs-N showed a better fluorescence sensing for Hg^{2+}, which is consistent with the above results for the four CDs solutions. In addition, the fluorescent hydrogel also showed an obvious fluorescence quenching for Hg^{2+} in the coexistence of multiple heavy metal ions (Fig. S9 in Supporting information). The excellent fluorescence quenching may be ascribed to the higher coordination interaction between Hg^{2+} and the functional groups of the CDs-N. Furthermore, the excellent mercury uptake capacity suggest that the CA/CDs-N hydrogel could be an effective sensor for environmental remediation (Fig. S10 and Table S5 in Supporting information).

In summary, the green synthesis of fluorescent CDs from C-CNC and dopants (urea, boron acid, glutathione) were achieved using a hydrothermal method. The four CDs synthesized exhibited good dispersion in aqueous solution and good fluorescence properties. Moreover, CDs-C, CDs-N, CDs-B and CDs-S were applied as the highly selective, sensitive, and effective sensors for the detection of Hg^{2+}. CDs-N was found to have a better sensitivity for Hg^{2+} with a detection limit of 8.29×10^{-6} mol/L, which was associated with the high affinity between the -NH_2 of the CDs-N and Hg^{2+}. DFT calculations further revealed that CDs-N preferred to absorb Hg^{2+} on the surface and they can form stable complexes. Based on its high-performance, the CDs-N were successfully used as fluorescence inks for anti-counterfeiting applications. Furthermore, the

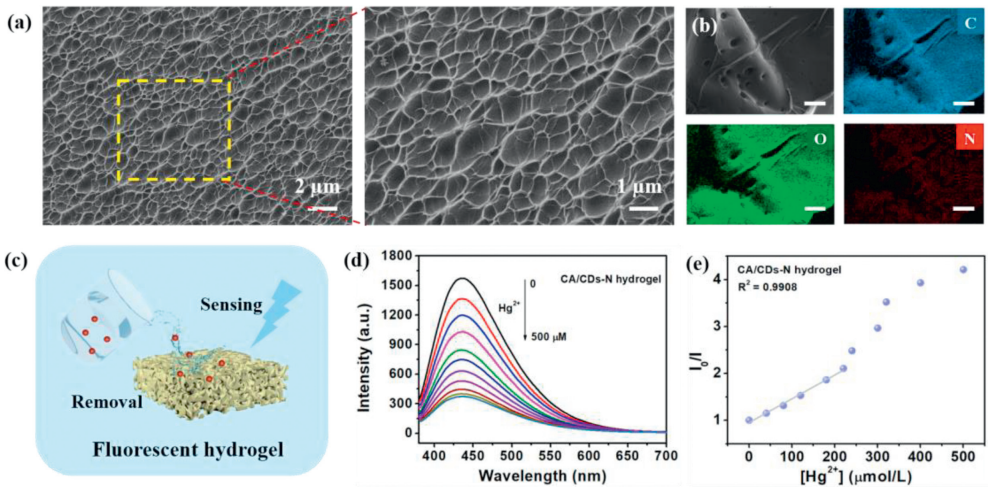

Fig. 4. Applications of fluorescent hydrogels. (a) SEM images and (b) EDS mapping of cellulose-based hydrogel. (c) Schematic of fluorescent hydrogel for the detection and adsorption of Hg^{2+}. (d) The fluorescence intensity of CA/CDs-N hydrogel for Hg^{2+}. (e) Fluorescence intensity ratios (I_0/I) of the CA/CDs-N hydrogel for Hg^{2+} (λ_{ex}= 360 nm).

fluorescent hydrogels containing CDs-N were used to detect and remove Hg^{2+}, revealing its potential in real world environmental applications. Moreover, the exhausted hydrogel materials can be vulcanized and then used for solar steam generation, realizing the sustainable development of materials. This study not only provides a green method for the preparation of CDs for the sensing of mercury ions, but also helps understand the fluorescence mechanism and the performance of CDs in existing technological applications.

Declaration of competing interest

Tony D. James has been appointed as a High-Level Foreign Expert by North China Electric Power University. Other authors declare that they have no known competing financial interests or personal relationships that could have appeared to influence the work reported in this paper.

Acknowledgments

The present work is supported by the National Natural Science Foundation of China (Nos. 52370110 and 21607044). This work was also supported by the Fundamental Research Funds for the Central Universities (No. 2023MS146) and the Open Research Fund of the School of Chemistry and Chemical Engineering, Henan Normal University for support (Nos. 2020ZD01 and 2021YB07). TDJ wishes to thank the Royal Society for a Wolfson Research Merit Award.

Supplementary materials

Supplementary material associated with this article can be found, in the online version, at doi:10.1016/j.cclet.2023.109021.

References

[1] M. Mokarram, A. Saber, V. Sheykhi, J. Clean Prod. 277 (2020) 123380.
[2] M. Santhamoorthy, K. Thirupathi, D. Thirumalai, et al., Environ. Res. 212 (2022) 113211.
[3] D. Kou, W. Ma, S. Zhang, Adv. Funct. Mater. 31 (2021) 2007032.
[4] Y. Yang, Y. Zhao, W. Shi, et al., J. Lumin. 209 (2019) 102–108.
[5] H. Guo, L. Peng, N. Wu, et al., Colloid. Surface A 634 (2022) 128023.
[6] M. Li, X. An, M. Jiang, et al., ACS Sustain. Chem. Eng. 7 (2019) 15182–15189.
[7] L. Miao, W. Liu, Q. Qiao, et al., J. Pharm. Anal. 10 (2020) 444–451.
[8] X. Li, J. Zheng, W. Liu, et al., Chin. Chem. Lett. 31 (2020) 2937–2940.
[9] W. Zhou, X. Fang, Q. Qiao, et al., Chin. Chem. Lett. 32 (2021) 943–946.
[10] F. Yan, X. Zhao, R. Li, et al., Chin. Chem. Lett. 35 (2024) 108504.
[11] Y. Fu, S. Wu, H. Zhou, et al., Ind. Eng. Chem. Res. 59 (2020) 1723–1729.
[12] X. Li, S. Zhao, B. Li, et al., Coord. Chem. Rev. 431 (2021) 213686.
[13] X. Li, X. Xing, S. Zhao, et al., Chin. Chem. Lett. 33 (2022) 1632–1636.
[14] Y. Zhang, H. Xiao, R. Xiong, C. Huang, Sep. Purif. Technol. 324 (2023) 124513.
[15] S. Mohandoss, N. Ahmad, M.R. Khan, et al., Environ. Res. 228 (2023) 115898.
[16] S. Liao, L. Zhang, S. Li, et al., New J. Chem. 47 (2023) 14242–14248.
[17] R. Reshmy, E. Philip, A. Madhavan, et al., J. Hazard. Mater. 424 (2022) 127516.
[18] M. Li, Q. Tu, X. Long, et al., Int. J. Biol. Macromol. 166 (2021) 1526–1534.
[19] M.M. Langari, M.M. Antxustegi, J. Labidi, Chemosphere 302 (2022) 134823.
[20] M. Li, X. Li, M. Xu, et al., Chem. Eng. J. 426 (2021) 131296.
[21] J. Woo, Y. Song, J. Ahn, H. Kim, Cellulose 27 (2020) 4609–4621.
[22] A. Meng, Q. Xu, K. Zhao, et al., Sensor. Actuat. B: Chem. 255 (2018) 657–665.
[23] N. Sohal, S. Basu, B. Maity, Microchem. J. 185 (2023) 108287.
[24] B.P.d. Oliveira, N.U.d.C. Bessa, J.F. do Nascimento, et al., Int. J. Biol. Macromol. 227 (2023) 805–814.
[25] L. Luo, P. Wang, Y. Wang, F. Wang, Sensor. Actuat. B: Chem. 273 (2018) 1640–1647.
[26] H. Ding, S.B. Yu, J.S. Wei, H.M. Xiong, ACS Nano 10 (2016) 484–491.
[27] T. Gan, Y. Zhang, M. Yang, et al., Ind. Eng. Chem. Res. 57 (2018) 10786–10797.
[28] K.K. Karali, L. Sygellou, C.D. Stalikas, Talanta 189 (2018) 480–488.
[29] Y. Liu, P. Zhou, Y. Wu, et al., Sci. Total Environ. 827 (2022) 154357.
[30] M. Li, Q. Shi, N. Song, et al., Adv. Opt. Mater. 11 (2023) 2203079.
[31] M. Li, M. Yang, B. Liu, et al., Chem. Eng. J. 431 (2022) 134245.